Optimized spatial tool for the implementation of ground source heat pump coupled with photovoltaic panels heating systems in urban areas

Ramos-Escudero, Adela; Magraner, Teresa; Gil-García, Isabel C.

DOI
10.1016/j.enbuild.2024.114752

Publication date
2024

Document Version
Final published version

Published in
Energy and Buildings

Citation (APA)
Ramos-Escudero, A., Magraner, T., & Gil-García, I. C. (2024). Optimized spatial tool for the implementation of ground source heat pump coupled with photovoltaic panels heating systems in urban areas. *Energy and Buildings*, *323*, Article 114752. https://doi.org/10.1016/j.enbuild.2024.114752

Energy & Buildings 323 (2024) 114752

Contents lists available at ScienceDirect

Energy & Buildings

journal homepage: www.elsevier.com/locate/enbuild

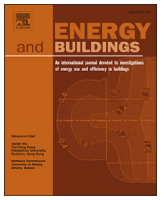

Optimized spatial tool for the implementation of ground source heat pump coupled with photovoltaic panels heating systems in urban areas

Adela Ramos-Escudero [a], Teresa Magraner [b], Isabel C. Gil-García [c,*]

[a] Water Management Department, Faculty of Civil Engineering and Geosciences, TU Delft, Stevinweg 1, 2600 GA, Delft, the Netherlands
[b] Dept. of Applied Thermodynamics, Universitat Politècnica València, Camino de Vera s/n, 46022, Valencia, Com. Valenciana, Spain
[c] Faculty of Engineering, Distance University of Madrid (UDIMA), C/ Coruña, km 38500, 28400, Collado Villalba, Madrid, Spain

ARTICLE INFO

Keywords:
Renewable heating systems
GIS
Ground source heat pump
Photovoltaic panels
MCDM

ABSTRACT

The growth of the urban population intensifies climate change due to the increase in activities that emit greenhouse gases, such as heating. However, proper urban planning and effective environmental policies can mitigate these impacts and foster a sustainable future. This study proposes an optimized spatial tool to implement renewable coupled heating systems in urban areas, combining geothermal heat pump technology with electricity generation through photovoltaic panels. The tool performs an exhaustive geospatial analysis that considers technical, economic, and socio-environmental criteria, offering multiple alternatives prioritized through multi-criteria evaluation methods. This facilitates the design of various scenarios according to the investment in renewable coupled systems for heating in buildings, in line with Sustainable Development Goals (SDG) 7, 11, and 13. The tool is evaluated in the city of Madrid, specifically in the neighborhood of Ciudad Lineal, generating a total of 2733 alternatives. Four scenarios are designed based on the annual subsidies provided by the Spanish Institute for Energy Diversification and Saving (IDAE) for heating and cooling using renewable energy sources. The first scenario, which includes 599 alternatives, manages to avoid emissions of 5 $MtCO_2$/year and primary energy savings of 278.9 GWh/year.

Nomenclature

Abbreviations

BHE	Borehole Heat Exchanger
Bi	Biomas
COP	Coefficient of heat pump performance
DHW	Domestic hot water
EED	Earth Energy Designer
GHG	Greenhouse Gas Protocol
GIS	Geographic Information Systems
GN	Natural gas
GSHP	Ground source heat pump
HVAC	Heating Ventilation Air Conditioning
IDAE	Spanish Institute for Energy Diversification and Saving
LCA	Lifecycle analysis
Mat	Construction materials
MCDM	Multi-Criteria Decision Making
NPV	Net present value
PV	Solar photovoltaic
PVT	Solar thermal
SCOP	Seasonal coefficient of performance in the heating season
SDG	Sustainable Development Goal
Thc	Thermoelectric cooler
TOPSIS	Technique for Order of Preference by Similarity to Ideal Solution
TRNSYS	Transient System Simulation Tool
URBAN3R	GIS based tool to support urban regeneration
Wi	Wind

Variables

E_{demand}	Building heating demand (kWh/year)
q	heat extraction (W/m)
t_{op}	Annual facility operation time (h)
l_{BHE}	Total length of vertical heat exchanger (m)
E_{GEN}	Energy generated annually (kWh)

* Corresponding author.
E-mail address: isabelcristina.gil@udima.es (I.C. Gil-García).

https://doi.org/10.1016/j.enbuild.2024.114752
Received 19 June 2024; Received in revised form 19 August 2024; Accepted 30 August 2024
Available online 4 September 2024

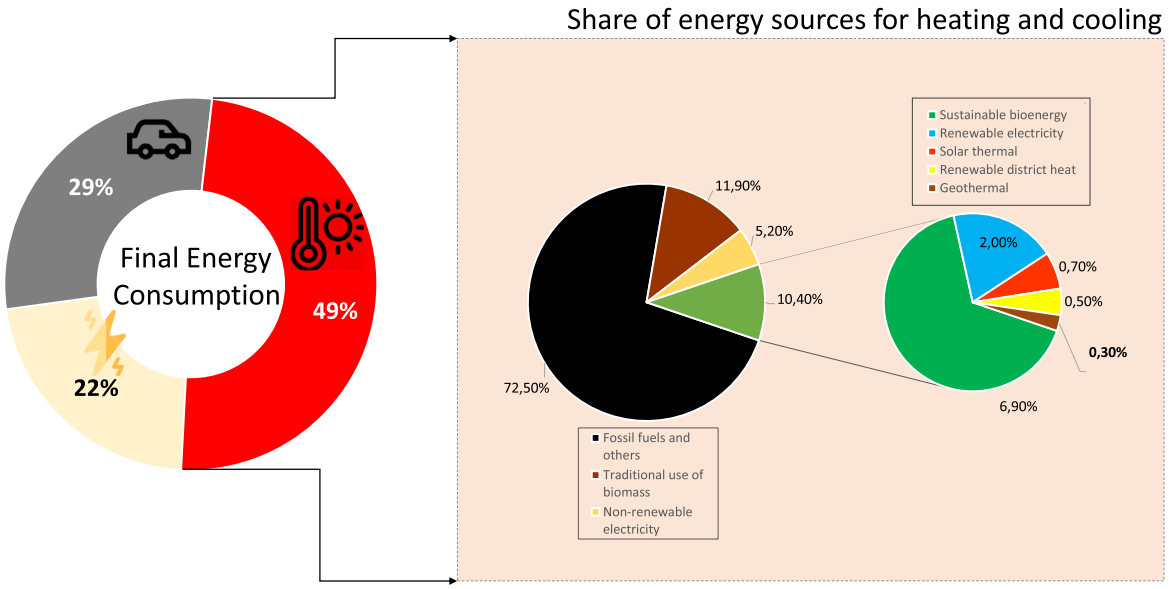

Fig. 1. Final Energy Consumption. Share of energy sources for heating and cooling. Data source [7]. Own elaboration.

PR	Performance Ratio of the PV panels
LT	Lifetime of the utility (years)
Pp	Power peak of the system (kW)
Irr	Solar irradiation (kWh/m^2 per year)
G_{STC}	Standard test conditions (STC) irradiance (1 kW/m^2)

1. Introduction

1.1. Background & significance

The challenge of climate change, driven predominantly by human activities that emit substantial amounts of greenhouse gases, stands as one of the foremost global issues of our time [1]. The goal of limiting temperature rise to below 1.5 degrees Celsius is pivotal, representing a critical effort to mitigate the most severe impacts of climate change [2]. Recent assessments indicate that global temperatures have already surpassed the 1.5 degrees Celsius threshold, emphasizing the urgent need for intensified climate action [3]. Urban areas are increasingly pivotal in this endeavor as they expand, heightening their vulnerability to climate risks and disasters. By the end of 2022, 57% of the global population, equivalent to 4.52 billion people, resided in urban settings [4], with this trend projected to persist. By 2050, the urban population is expected to double, with nearly seven out of ten individuals projected to live in cities [5]. Notably, the residential sector alone emits 1,989 million tons of CO_2 globally [6]. Regarding heating and cooling - including space heating and cooling in buildings, domestic hot water, cooking, industrial process heat, and agriculture, 49% of the total energy produced is consumed in heating. This sector constitutes the world's largest share of final energy consumption, surpassing electricity and transport. The origins of this energy are key to the climate crisis; fossil fuels and non-renewable electricity met more than 77% of heating and cooling demand, the use of modern renewables to meet heating and cooling needs has been limited to just over 10% of global demand, - including sustainable bioenergy, solar thermal and geothermal heat - met 6.9%, 0.7%, and 0.3% respectively of heating and cooling demand, and renewable electricity accounted for 2% [7], see Fig. 1.

Cities thus become crucial points for facilitating climate action, transitioning to sustainable energy sources, and promoting sustainability [8]. A number of targets are driving the transformation from fossil fuel-based heating and cooling systems to renewable hybrid or coupled systems. These targets, aligned with sustainable development goals [9], include efforts to reduce air pollution and its impacts on health, reduce greenhouse gas emissions, improve energy access, and address energy poverty. Renewable energies foster socio-economic benefits, leading to economic development and local employment [10]. The far-reaching potential of renewables in the field of heating and cooling is highlighted.

1.2. Literature review

During the period between 2020 and 2024, the authors carried out a comprehensive study on hybrid or coupled heating systems. This study focused on several fundamental aspects, including the technologies used in heating systems and objective indicators from technical, economic, and environmental perspectives. Additionally, the use of Geographic Information Systems (GIS) was explored to analyze the spatial distribution of these systems, multi-criteria evaluation methods were applied, and the direct relationship between heating systems and sustainable development goals was examined, see Table 1.

97% of works on hybrid-coupled systems incorporate solar photovoltaic or solar thermal technologies, while 80% include geothermal heat pumps. Regarding multicriteria evaluation methods, Chen et al. [13] analyze the optimal hot water allocation ratio to maximize the hybrid system's performance in a specific building, considering energy factors. On the other hand, Ren et al. [20] employ the TOPSIS method to determine the ideal solution among a group of alternatives, considering different infrastructures, operational strategies, hybrid systems, and objective indicators in terms of energy efficiency, environmental impact, and economic viability. Similarly using the TOPSIS method, a dynamic model was developed that integrates solar energy, geothermal energy, and energy storage, optimized with a genetic algorithm. In a case study in Beijing, the optimized system outperformed the reference system, achieving a 69% performance index and 79% renewable energy utilization [47]. A multi-energy complementary heating system was developed in rural areas using renewable energy. The entropy-TOPSIS method was employed to evaluate and optimize the system's operation, establishing six working modes. Results indicated that the optimal energy supply mode for maximizing heating efficiency was the combination of solar and biomass energy [49].

40% of the works include technical, economic and environmental indicators, among them we highlight the following. Kavian et al. [12] proposed a hybrid photovoltaic-geothermal system to meet the heating and cooling demands in a residential building. This system, analyzed using a numerical dynamic model that considers various components such as solar panels, batteries, inverters, and geothermal heat

Table 1
Previous studies focused on hybrid or coupled systems for heating. Overview of factors analyzed and comparison with this study. Legend-Column: *Hybrid-coupled systems* (PV: solar photovoltaic, PVT: solar thermal, GSHP: ground source heat pump, Bi: biomass, Wi: wind, GN: natural gas, Thc: thermoelectric coolers, Mat: construction materials). Column: *Objective Indicators* (T: Technical, E: Economic, A: Environmental).

Ref.	Year	Hybrid-coupled System	GIS	MCDM	Objective Indicators	ODS
[11]		PV-PVT-GSHP-Wi			T,A	
[12]		PV-GSHP			T,E,A	
[13]	2020	GSHP-GN			T	
[13]		PV-PVT-GSHP		✓	T,E,A	
[14]		PV-GSHP			T,A	
[15]		PV-PVT-GSHP			T,A	
[16]		PV-GSHP			T	
[17]		PV-PVT-GSHP			T	
[18]	2021	PV-GSHP			T,E	
[19]		PV-GSHP			T,E,A	
[20]		PV-PVT-GSHP		✓	T,E,A	
[21]		PV-PVT-GSHP			T,A	
[22]		PV-PVT-GSHP			T,E	
[23]		PV-GSHP			T,E,A	
[24]		PV-GSHP			T,E,A	
[25]		PVT-GSHP			T,A	
[26]		PV-GSHP			T,E,A	
[27]	2022	PV-GSHP			T,E	
[28]		PV-GSHP			T,E	
[29]		PV-PVT-GSHP			T,A	
[30]		PV-GSHP			T,E	
[31]		PV-GSHP			T,E,A	
[32]		PV-Mat			T,E	
[33]		PV-GSHP			T,E	
[34]		PV-GSHP-Bi			T,E,A	
[35]		PV-GSHP			T,E,A	
[36]		PV-PVT-Wi			T,E	
[37]	2023	PVT-GSHP			T,E	
[38]		PV-Thc			T,E	
[39]		PVT-GSHP			T,E	
[40]		PV-GSHP			T,E	
[41]		PV-GSHP			T,E,A	
[42]		PV-GN-Thc		✓	T,A	
[43]		PV-Bi			T,E,A	
[44]		PV-Mat			T,E,A	
[45]	2024	PV-PVT-GSHP			T	
[46]		PVT-GSHP-Bi			T,E,A	
[47]		PVT-GSHP-GN		✓	T,E,A	
[48]		PVT-Bi			T,A	
[49]		PVT-Bi		✓	T,E,A	
This Paper		PV-GSHP	✓	✓	T,E,A	7,11,13

pumps, was optimized to minimize costs and maximize efficiency using a particle swarm optimization algorithm. The study revealed that the polycrystalline hybrid photovoltaic system, with a surface area of 35 m^2 and a solar fraction of 31%, was profitable even with an inflation rate of 24%. On the other hand, and in the same line of specific cases, Perkovc et al. [19] explored the effectiveness of decarbonizing the household sector through the consumption of microgrids, merging renewable sources for electricity, heating, and cooling. Their analysis of a hypothetical microgrid in Zagreb integrating photovoltaic and geothermal energy demonstrated a balance in energy flows and a notable reduction in CO_2 emissions. The close integration between energy demand and supply promotes profitable decarbonization in the domestic sector. Solar-assisted ground source heat operation has been analyzed by Nahavandinezhad and Zahedi [23] in four different configurations: GSHP supplying heating, cooling, and DHW and PV panels providing the necessary electricity; PVT panels installed in parallel with GSHP to provide heating and DHW instead of the heat pump in order to reduce the heat pump operation; GSHP and PVT panels installed in series through an external exchanger using the source with the most appropriated temperature, and a direct design in which the solar collector and the GSHP exchanged heat directly with each other enhancing the performance of the PVT. These configurations have been evaluated and compared technically, economically, and environmentally, concluding that the last option is the best hybrid system for the location analyzed with an investment return of 7 years. PVT and GSHP hybridization has also been studied by Pilou et al. [24], in this case, applied for heating and cooling an office building. The analysis is carried out in two locations (Athens and Copenhagen) considering three thermal demand scenarios (high, medium, and low), depending on the number of PTV panels installed, the COP of the heat pump, the electricity demanded by the system, and the PVT electricity production. The main result of this work is that it presents a system capable of achieving a renewable energy share between 75-80% in office buildings located in southern Europe and between 50-60% in buildings in northern Europe, reducing GHG emissions and increasing self-consumption. In [31], Calise et al. perform a thermoeconomic analysis of a solar driven 5th generation district heating and cooling network coupled with water to water and ground source heat pumps. The system proposed, and its operation strategies are modeled in TRNSYS, particularly in a case study that supplies 50 buildings located in Leganés (Madrid, central Spain). Network energy performance

is assessed through the primary energy demand and a primary energy saving index relative to a reference system (natural gas boilers for heating and DHW and electrically driven air-to-air heat pumps for cooling). A primary energy saving index of 64% is obtained for the optimal photovoltaic field area although corresponds to a high payback period of 33 years. A feasibility evaluation of multi-energy hybrid systems combing different renewable energy sources applied a several buildings of the Olympic Training Center in Kuortane (Finland) is performed by Lü et al. [34]. This work aimed to obtain the best renewable combination (deep and shallow geothermal, biomass, and solar PV or electricity grid as complementary energy) to replace the peat-fired boiler, considering both thermal demand and the evolution of electricity market prices. A lifecycle analysis (LCA) is carried out to obtain the lifecycle (NPV) profitability indicator for the different options evaluated. In conclusion, it is deduced that geothermal energy alone is not a viable technology compared to biomass, but if the peak loads can be reduced by electricity, purchasing from the grid becomes an economical option. The combination of GSHP systems and PV panels to achieve net zero-emission buildings is analyzed in [41], Kim and Junghans use the TRNSYS software tool to simulate different HVAC systems in a residential building, comparing the air source heat pump with the ground source heat pump, both supplied by a PV installation. Three critical aspects are calculated to analyze the energy rates to meet the objective of net zero-emission: grid energy demand, building operation cost, and GHG emissions. For the option PV panels integrated with GSHP system, energy conversion rates reach 24,75%, 28,50% and 43,50% in these indicators. Billerbeck et al. [46] presents a European energy model that integrates district heating with high spatial resolution for 25 EU Member States in 2050. It highlights the use of renewable sources and excess heat, finding that heat pumps and geothermal energy offer cost advantages for heating generation.

The primary innovation of this paper stems from the notable absence of studies addressing the integration of spatial analysis with hybrid heating systems. Despite extensive research in the field of urban energy systems, the authors did not identify any work that combines these aspects, nor did they find research specifically aligned with the Sustainable Development Goals (SDGs). This highlights a significant scientific gap and knowledge deficit. To address this, the present study develops a novel tool that not only facilitates the efficient and sustainable planning of heating infrastructure but also directly contributes to achieving SDGs 7, 11, and 13. This innovative approach bridges the existing gap in the literature, offering a comprehensive framework for sustainable urban energy solutions.

1.3. Motivation & contributions

In this context, the motivation behind this work stems from the need for efficient and sustainable solutions in urban energy systems [50]. Urban areas are particularly challenged by high energy demands and significant greenhouse gas (GHG) emissions, necessitating innovative approaches to improve sustainability Marvuglia et al. [51]. A spatial planning tool has been developed to facilitate the efficient and sustainable implementation of coupled geothermal heat pump (GSHP) and photovoltaic (PV) systems. This tool leverages geospatial analysis and multi-criteria evaluation, enabling detailed and adaptable assessments tailored to specific urban contexts. By providing a robust framework for informed decision-making in heating infrastructure planning, the tool addresses key challenges such as the assessment of the availability of space for drilling the Borehole Heat Exchanger (BHE) required, cost variability, and limited space for PV installation.) Under this framework, the present study aims to develop an optimized spatial tool for implementing renewable heating systems in urban areas, specifically combining geothermal heat pump technology with on-site electricity production using photovoltaic panels. Thus, the key question that this work addresses is how a novel tool for the spatial planning of renewable systems, incorporating geospatial analysis and multi-criteria evaluation, facilitates efficient and sustainable heating infrastructure planning in urban areas while addressing specific zone characteristics and overcoming challenges such as interior building space assessment and cost variability. The main contributions of this work are:

- It provides a tool that facilitates efficient and sustainable planning of heating infrastructure, combining various renewable energy sources and adapting to urban environments' specific characteristics and needs.
- It conducts a comprehensive spatial analysis, moving beyond individual and simplistic approaches that cannot be generalized to other areas, thus enhancing the tool's applicability and robustness.
- It incorporates technical, economic, environmental, and social criteria into the tool's modeling, aligning with political initiatives to improve energy security and achieve climate objectives.
- It directly contributes to sustainable development goals 7 (affordable and clean energy), 11 (sustainable cities and communities), and 13 (climate action).

The evaluation of the model is based on a real area of Spain; the rest of the document is organized as follows. The methodological proposal is described in section 2. The evaluation of the tool is in section 3. The results and discussion are in section 4. Finally, conclusions are given in section 5.

2. Proposed methodology

The proposed methodology encompasses three stages: (*i*) Input (*ii*) Modeling, and (*iii*) Output, as depicted in Fig. 2.

2.1. Phase 1. Input

2.1.1. Geographic information system (GIS) assessment

In this study, GIS plays an essential role, enabling a comprehensive assessment through the use of open-access QGIS v.3.32.3 [52]. GIS facilitates several critical processes. All information is organized into thematic layers, with each piece of data geospatially localized. GIS is used to analyze geospatial databases, including natural resource features (geothermal and solar), land use, and building information. New information, such as geothermal and solar potential, is produced based on spatial data modeling. Additionally, suitable locations are identified by integrating the newly generated information with collected data.

The assessment includes analyzing restriction layers to determine suitable areas for the study. This analysis identifies the appropriate space for drilling the BHE field in urban areas. For the initial selection, restricted and permitted areas are delineated within the urban zones.

2.1.2. Selecting suitable areas: restrictions and permissions

In the proposed location problem, the selection of suitable surface areas and buildings within the urban area is determined by identifying and excluding restricted spaces using a GIS tool. Restrictions are defined by factors such as public transport infrastructure (primarily subways), buffer zones around buildings, and other protected urban areas. Once the restricted areas are excluded, suitable areas are selected based on the identification of permitted spaces where drilling is allowed, the proximity of nearby buildings, and the availability of sufficient space for the BHE. Permitted areas are chosen from free spaces near buildings, such as parks, city gardens, pavements, and backyards. However, not all buildings are considered; they must meet the following conditions: Maintain a safety distance from the building and surrounding infrastructure; Have a considerable space (greater than 500 m^2); Be within 5 m of the building to reduce hydraulic losses and minimize pumping costs. Both the restrictions and permitted parameters are defined using thematic layers, which can be obtained from open or non-open access databases, government organizations at the municipal or national level, or companies specializing in spatial information processing. By using QGIS software

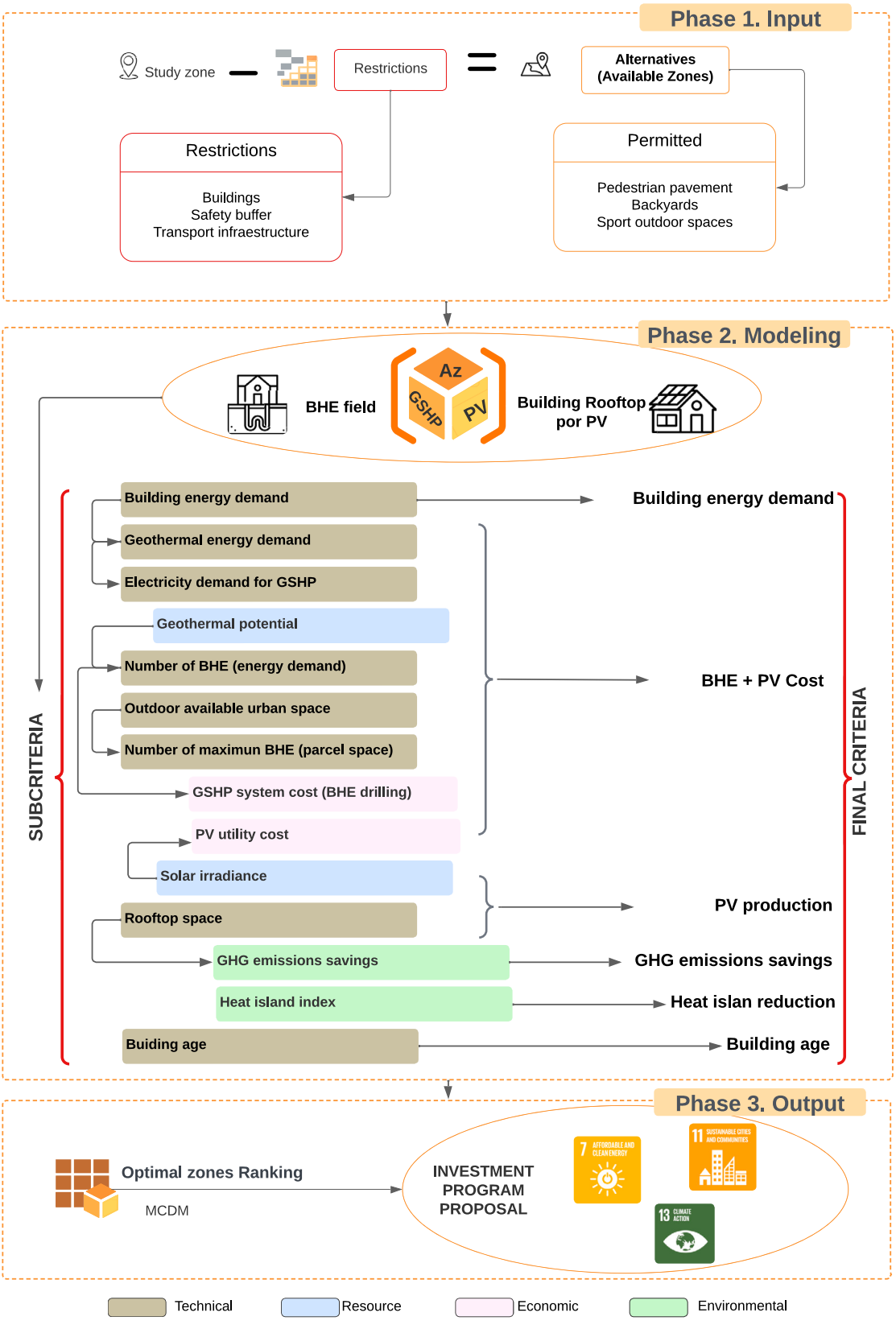

Fig. 2. Architecture of the proposed methodology.

to subtract thematic layers that define each restriction from the original layer covering the entire study area, suitable areas for implementing coupled geothermal-PV systems for individual buildings can be identified.

2.2. Phase 2. Modeling

The determination of each criterion involves a combination of scientific analysis, empirical data collection, and expert judgment. Upon identifying and refining the study area, thematic layers defining the criteria are integrated as inputs in QGIS. Some thematic layers are directly collected and used, while others are calculated using GIS tools. The selection of the final criteria takes into account, both directly and indirectly, the technical, economic, resource, and environmental potential of the different parameters affecting the decision on optimal zones (see Fig. 2). During this phase, the assessment process for optimal locations continues; buildings that do not meet the criteria are systematically excluded. The criteria and the process for their assessment are described in detail in the following sections 2.2.

2.2.1. Building energy demand

It is considered a technical criterion, and it assesses the energy demand of the buildings needed to provide space heating within the urban area. The determination of the total energy demand can be simulated with different simulation tools (i.e. TRNSYS [53], EnergyPlus [54], ESP-r [55], etc.), or can be collected from databases. Target buildings are those beneficiaries of energy refurbishment investment programs, such as residential buildings, as they may benefit from coupled geothermal-PV systems.

2.2.2. Number of borehole heat exchangers (BHE)

The assessment of the number of boreholes involves two main considerations: Firstly, determining the maximum number of boreholes feasible per available parcel near a building. This serves as an initial filter to evaluate each parcel's availability and potential as a BHE field. Secondly, establishing the number of boreholes required to meet a building's specific thermal demand. This evaluation assesses the suitability of a parcel in relation to its association with a particular building's energy needs. It directly relates to the feasibility and efficiency of implementing geothermal systems. Different subcriteria are considered to obtain this criterion, which are explained below. The geothermal potential based on the underground conditions and the thermal conductivity seems to be the most important. However, is assumed that both are constant throughout the reduced area and thus cannot be considered as a criterion to make a distinction in the optimal selection problem. They are considered in the system cost criteria, as explained later. The space availability is another important subcriteria considered. They are the outdoor free spaces available that are not far from the specific building, which is more than 5 m, to avoid hydraulic losses from the horizontal geothermal loop. To obtain the maximum number of BHEs available for every building, the surface of the free space is divided by the area required by every BHE, considering the safety space between themselves, which can vary from one study case to another. The number of BHE required has been calculated from the heating demand obtained from the buildings databases, the heat extraction rate, the facility operation time determined from the annual hours in which heating is necessary because the outside temperature is below a certain value applying a use factor and the seasonal coefficient of performance of the heat pump ([56]).

$$E_{demand} * (1 - 1/SCOP) = q * t_{op} * l_{BHE} \quad (1)$$

Where E_{demand} is the building heating demand (kWh/year), SCOP is the seasonal coefficient of performance in the heating season, q is the heat extraction rate (W/m), t_{op} is the annual facility operation time (h) and l_{BHE} is the total length of vertical heat exchanger (m). By setting a borehole depth of 100 m (single U-pipe), the number of BHE to cover the building's heating demand is obtained. The number of boreholes that can be drilled in the urban areas is assessed using GIS in different steps. Firstly, the parcels located near the buildings (maximum 5 m distance) available for drilling the BHE must be identified and divided into different buildings. Then, to calculate the maximum number of BHEs per parcel and building (2) is applied.

$$Numberof\,BHE = Parcel\ area/(Savety\ distance)^2 \quad (2)$$

This is possible by overlapping the building polygons with BHE available area polygons and, ultimately, the number of BHE.

2.2.3. Electricity production from the PV panels

To estimate the maximum electricity generated per building by the hypothetical PV system, (3) is applied ([57]).

$$E_{GEN} = PR * LT * Pp * (Irr/G_{STC}) * Rooftopsurface \quad (3)$$

Where E_{GEN} is the energy generated annually (kWh), PR is the Performance Ratio of the PV panels, LT the lifetime of the utility (years), Pp is the Power peak of the system (kW), Irr is the solar irradiation (kWh/m^2 per year), the G_{STC} is the standard test conditions (STC) irradiance: 1 kW/m^2, and finally, the Rooftop surface is the usable surface available for every building to install the PV panels. Thus, the potential of the rooftops to provide electricity for the GSHP is assessed based on the space available, the shading, and the solar irradiance. Some subcriteria that cannot be assessed spatially are not considered, such as the rooftop technical suitability to installing the panels or the orientation.

2.2.4. Coupled system cost

This criterion includes the cost of the geothermal system plus the cost of the PV system per square meter of building. This criterion tackles the economic feasibility of the system. The conditions stated here are: the system consider covers 100% of the total thermal energy demand, and the PV system cover the electricity that the GSHP demand entirely. The building that do not fulfill these conditions are deleted. Once the thermal energy demand and the number of BHE are known, the cost of the geothermal system can be assessed based on the price databases of the studied area. The cost per linear meter of BHE includes the total investment in the installation. In the same way, the cost for the PV system is established per m^2 of panel installed.

2.2.5. Emissions saved

The primary focus here is to assess the reduction in greenhouse gas emissions and primary energy consumption resulting from the coupled of a photovoltaic (PV) solar installation with a geothermal system. We specifically exclude considerations of savings derived from geothermal use compared to alternative heating technologies such as aerothermal or conventional boilers. Our objective is to estimate the potential reduction in greenhouse gas emissions achieved by displacing conventional energy sources with renewable energy generation, specifically geothermal and PV, and to evaluate the environmental competitiveness of this integrated system. The assessment of emission savings involves a two-stage calculation process. Initially, we compute the electricity required by the heat pump for each building, subtracting the electricity that the building can generate through photovoltaic (PV) systems (from 2.2.3). This is calculated based on the building's heating demand and the heat pump's efficiency (Coefficient of Performance or COP). This approach allows us to quantify the net electricity demand met by the geothermal-PV coupled system, thereby facilitating a precise estimation of emission reductions attributable to renewable energy displacement ($KgCO_2$).

2.3. Output

2.3.1. Selection of optimal zones with MCDM

To identify the optimal conditions for a GSHP-PV system within urban areas, Multi-Criteria Decision Making (MCDM) methods are employed. The process begins with the matrix derived from phase 2, which

captures the relationship between criteria and the areas or alternatives under study. These alternatives represent buildings identified through GIS after applying the selection criteria. Various methodologies are employed to effectively classify these alternatives [58]. Typically, criteria weights are assigned to prioritize their relative importance, and alternatives are then ranked accordingly [59]. The entropy method for determining weights in multi-criteria decision-making is a technique that uses information theory; it provides an objective way to assign importance to criteria [60]. Its objective is to assign weights to the criteria equitably and objectively. Here is a summary of the process [61]:

1. Data normalization: The values of the criteria are adjusted so that they are comparable to each other, eliminating scale differences.
2. Entropy calculation: The entropy of each criterion is determined using Shannon's entropy formula. Entropy is interpreted as a measure of uncertainty or dispersion in the criterion values. The greater the entropy, the greater the uncertainty.
3. Calculation of relative information: The relative information is calculated for each criterion, dividing the entropy of the criterion by the total sum of entropies of all the criteria. This provides a measure of the relative importance of each criterion in relation to the others.
4. Weight assignment: Weights are assigned to the criteria using the calculated relative information. Criteria with lower entropy (lower uncertainty) obtain greater weight in decision-making.
5. Normalization of weights: The weights are adjusted so that they add up to 1, thus ensuring an adequate distribution of the importance of the criteria.

The VIKOR method, which stands for "Multi-Criteria Compromising Optimization," is a technique used to rank alternatives based on multiple criteria, taking into account both performance close to the ideal solution and distance to the anti-ideal solution [62]. Here is a summary of the process [63]:

1. Data normalization: The criteria values are normalized to eliminate scale differences and allow direct comparison between them.
2. Determination of weights: Weights are assigned to the criteria according to their relative importance in decision-making. These weights can be provided by experts or calculated using analytical methods such as entropy.
3. Alternative score calculation: A score is calculated for each alternative using a weighted combination of the normalized criteria values and the assigned weights.
4. Identification of the ideal and anti-ideal solutions: The best and worst alternatives for each criterion are determined based on their normalized values. The ideal solution is one that maximizes benefits and minimizes costs, while the anti-ideal solution is the opposite.
5. Calculation of the distance to the ideal solution and the anti-ideal solution: The distance between each alternative and the ideal solution and the anti-ideal solution, respectively, is calculated using some measure of distance, such as the Euclidean distance.
6. Calculation of the agreement and disagreement index: The agreement and disagreement indices are calculated for each alternative based on its distance from the ideal and anti-ideal solutions. The concordance index measures how close an alternative is to the ideal solution compared to other alternatives, while the discordance index measures how far an alternative is from the anti-ideal solution compared to other alternatives.
7. Calculation of the classification index: A classification index is calculated for each alternative, which combines the agreement and disagreement indices into a single measure.
8. Sorting of alternatives: Alternatives are sorted based on their ranking indices so that those with lower indices (indicating better performance) are placed at the top of the list.

2.3.2. Investment program proposal

Alternatives ranking is used to prioritize the most suitable investment (public and private) in building energy refurbishment projects. In this way, knowing the annual budget, the number of buildings in which actions will be carried out can be determined following the ranking obtained by applying the developed methodology establishing the investment program. This is very useful for urban planners who can allocate available resources to projects that are technically viable, involve greater savings in primary energy and greenhouse gas emissions and require less investment.

3. Study case

Ciudad Lineal is a neighborhood of Madrid, Spain that accounts for generous outdoor spaces and is densely populated, which converts it into an optimal study case for such systems in a big urban zone, see Fig. 3. Ciudad Lineal accounts for a total surface of 11.4 km^2 (604.3 km^2 total Madrid) and a population density of 87 inhabitants/Ha, which is above the municipal average (52 inhabitants/Ha). Madrid city represents 15% of the total population of Spain and has an average temperature of $14{,}3°C$ and an annual temperature amplitude of $36°C$ with a continental climate ([64]).

3.1. Phase 1. Input

To select the available space required by the coupled system, both permitted and restricted areas within the city environment were studied. Permitted zones for the BHE field encompass pedestrian pavement spaces and recreational areas such as green spaces, sports facilities, and outdoor areas adjacent to buildings. This information is openly accessible and was collected from the Opendata Madrid Municipality database [65] in a shapefile format. Buildings, though, serve as the primary constraints on land use for the BHE field, delineating areas where construction and other activities may be restricted or regulated. Restricted zones thus include buildings and a 3 m buffer zone (Spanish standard UNE 100715-1 [66]) around them, as well as transportation infrastructure, mainly metro lines. Building information was extracted from the [66]. As a result, a total of 355 Ha contained in 1,864 parcels that range from 1 to 139,6000 m^2 (green areas in Fig. 4a and brown areas in Fig. 4b) seem to be suitable to drill BHE. The space on the selected buildings' rooftops was considered the available space for PV panels. This information was collected from the [67]. The 6,855 buildings selected seem to offer a total of suitable 259 Ha of space in the roof, in principle, available for PV panels, with an average of 378 m^2 each.

3.2. Phase 2. Modeling

3.2.1. Building energy demand

To characterize buildings' energy demand, the URBAN3R database has been used ([68]). This database provides heating demand data by square meter, collecting the values of the energy performance certificates carried out by the methodology indicated in the Energy Performance of Buildings Directive ([69]). Most of the buildings in the neighborhood were built between the 1940s and the 1980s, which implies that their energy efficiency is low, with energy ratings on a scale from G (least efficient) to A (most efficient) between F and D. Of the total buildings analyzed, 32% were built between 1941 and 1960 and 44% between 1961 and 1980. The former has an average heating demand of 110.5 kWh/m^2 year, and the latter 76.8 kWh/m^2 year; a range that represents the characteristic heating demand of 80% of the buildings in the neighborhood is 182.4 - 71.0 kWh/m^2 year. Buildings after 1980 and before 2007, built with the NBE-CT-79 Spanish law ([70]), represent 19% of the total, and have an average heating demand of 50.7 kWh/m^2 year. The newest buildings, built after the approval of the Technical Building Code in 2006 ([71]) and until 2020, represent less than 2% of the real estate stock and have an average heating demand of 36.5 kWh/m^2 years.

Fig. 3. Study case. Ciudad Lineal Neighborhood, Madrid - Spain.

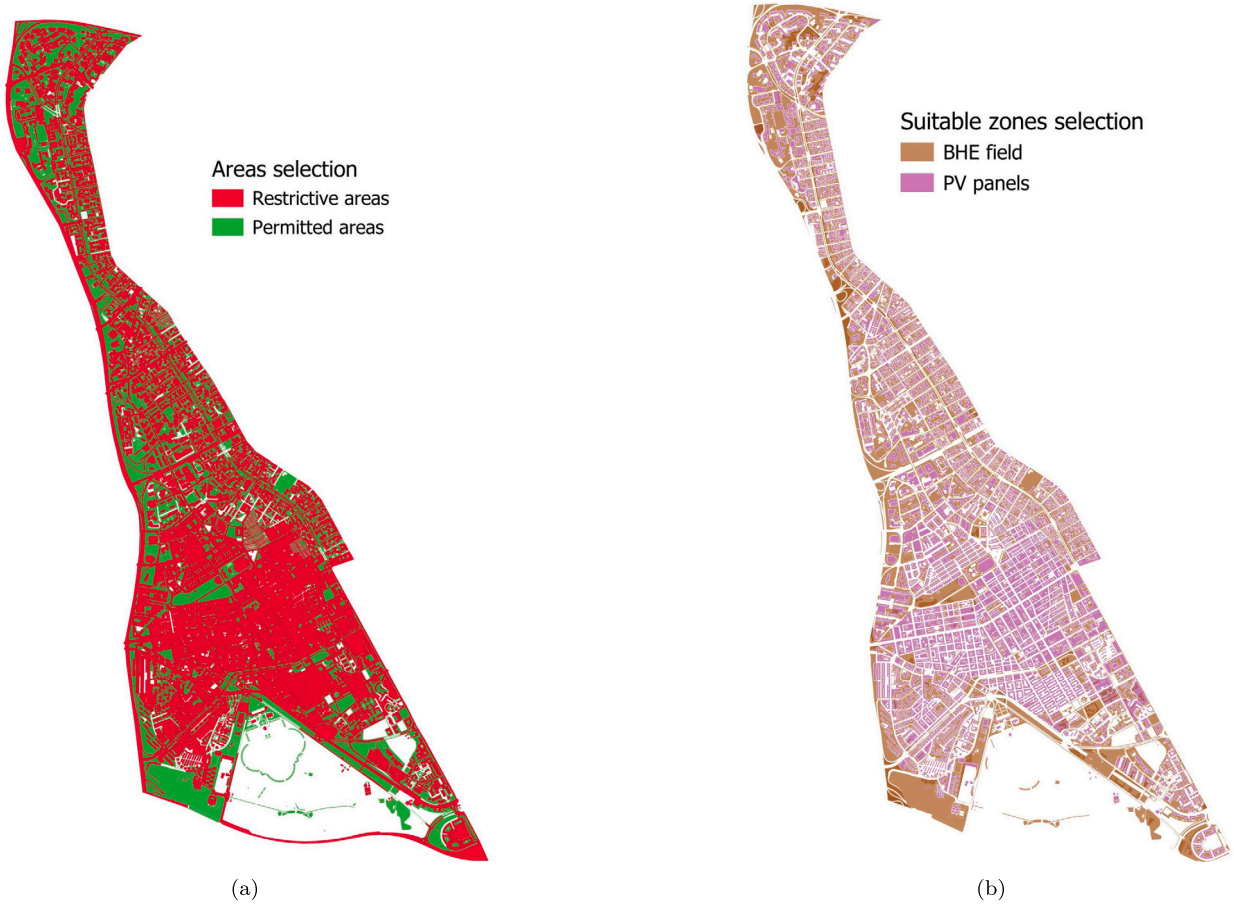

Fig. 4. (a) Restrictive and permitted areas for BHE field, (b) Available zones for BHE field and PV panels. (For interpretation of the colors in the figure(s), the reader is referred to the web version of this article.)

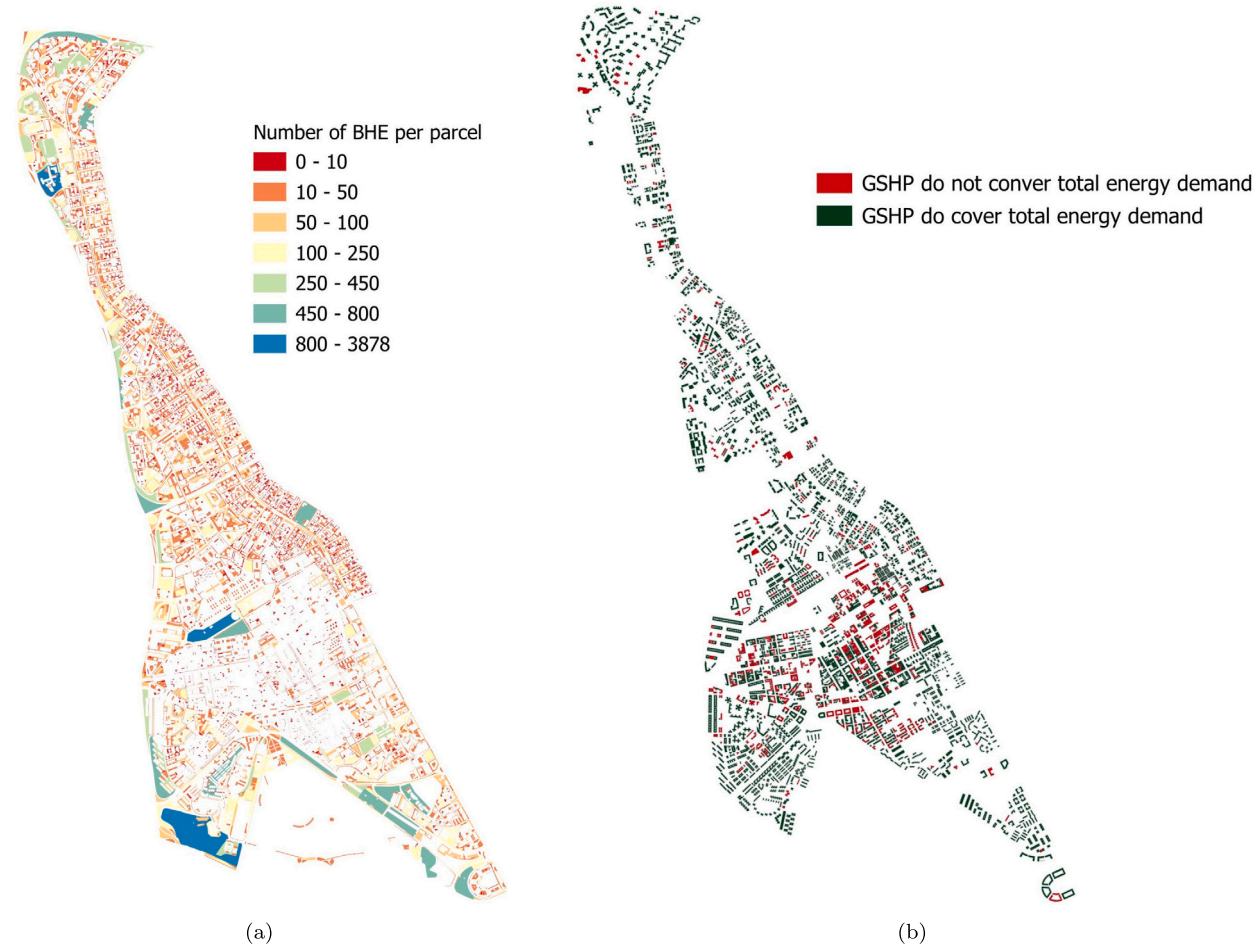

Fig. 5. (a) Maximum number of BHE that can be accommodated per parcel (b) Buildings that could allocate enough BHE to provide utterly the energy demand with shallow geothermal (green areas), and parcels that do not (in red).

To obtain the annual heating demand of each building, it has been considered that 80% of the surface given by the cadastre database is heated to exclude common areas.

3.2.2. Number of boreholes heat exchangers

Once building heating demand has been obtained, the number of borehole heat exchangers needed for each building has been calculated using (2). A conservative SCOP value of 3.0 has been considered in the calculations because it is a value that meets the regulatory requirement to consider the heat pump as renewable energy (SCOP $\geq$ 2.5) ([72]) and also it is a value that is reached by most of the equipment available on the market, even for the supply at high temperatures to terminal units such as radiators, an aspect to take into account when replacing boilers by heat pumps in energy refurbishment projects. The Madrid region's shallow geothermal power map ([73]) establishes a heat extraction rate between 35-50 W/m in the study area. The lower value has been used in the calculations, which has been verified using the EED program ([74]) carrying out a representative case of the neighborhood (133 kWh/m^2 year of heating demand) considering the following data: ground thermal conductivity (2.22 W/mK), ground volumetric heat capacity (2.3 MJ/m^{3}K) [75], undisturbed ground temperature (17°C), single U-pipes and monoethylenglycole at 14% as a heat transfer fluid, obtaining a heat extraction rate of 39 W/m, close to the used value of 35 W/m, for an annual heating demand of 156,570 kWh/year and a BHE total length of 3,000 m. To calculate the operation time, the number of hours in which the outside temperature is less than 15 °C during heating season has been determined from the climate database, assuming that the heating system is on when the outside temperature is below 15°C, a valid hypothesis for buildings with low internal thermal load, 24-hour use and heating setpoint temperature around 21 ºC ([76]). According to ([64]), in Madrid, there are 4043 hours a year with temperatures below 15 ºC between November and April. Considering that the heat pump will not always be operating when heating is requested, a use factor of 0.21 was calculated from the data of the representative case carried out. The selected BHE drilling sites were identified based on proximity to nearby buildings within a radius of no more than $3m$; see Fig. 4b. Each building was then associated with the available nearby area. In cases where one parcel was shared among multiple buildings, it was divided accordingly. A total of 176,623 BHE must be drilled to cover the total energy demand of the buildings. Considering the 6,173 buildings in the study area, that means 28 BHE as average, however, 7 is the most frequent number of BHE required per building.

Additionally, an estimation was made of the maximum number of BHE that could be drilled per parcel, see Fig. 5a. This analysis provides insights into the capacity of each parcel to accommodate the necessary BHEs to meet thermal demands comprehensively. Across the 1,863 selected parcels covering a total area of 375 hectares, a maximum of 104,088 BHEs could be drilled, averaging 17 BHEs per parcel. However, practical constraints such as distances between parcels and buildings restrict the utilization of available areas for BHE installations. Among the initially selected 6,060 parcels, approximately half (3,082 parcels) can effectively accommodate BHE installations, while the remainder (2,978 parcels) cannot be utilized due to distance limitations from buildings. These 3,082 parcels could provide shallow geothermal energy to 4,585 buildings, from which 3,798 buildings (82% of buildings), see Fig. 5b, might be capable of meeting 100% of their energy demands through

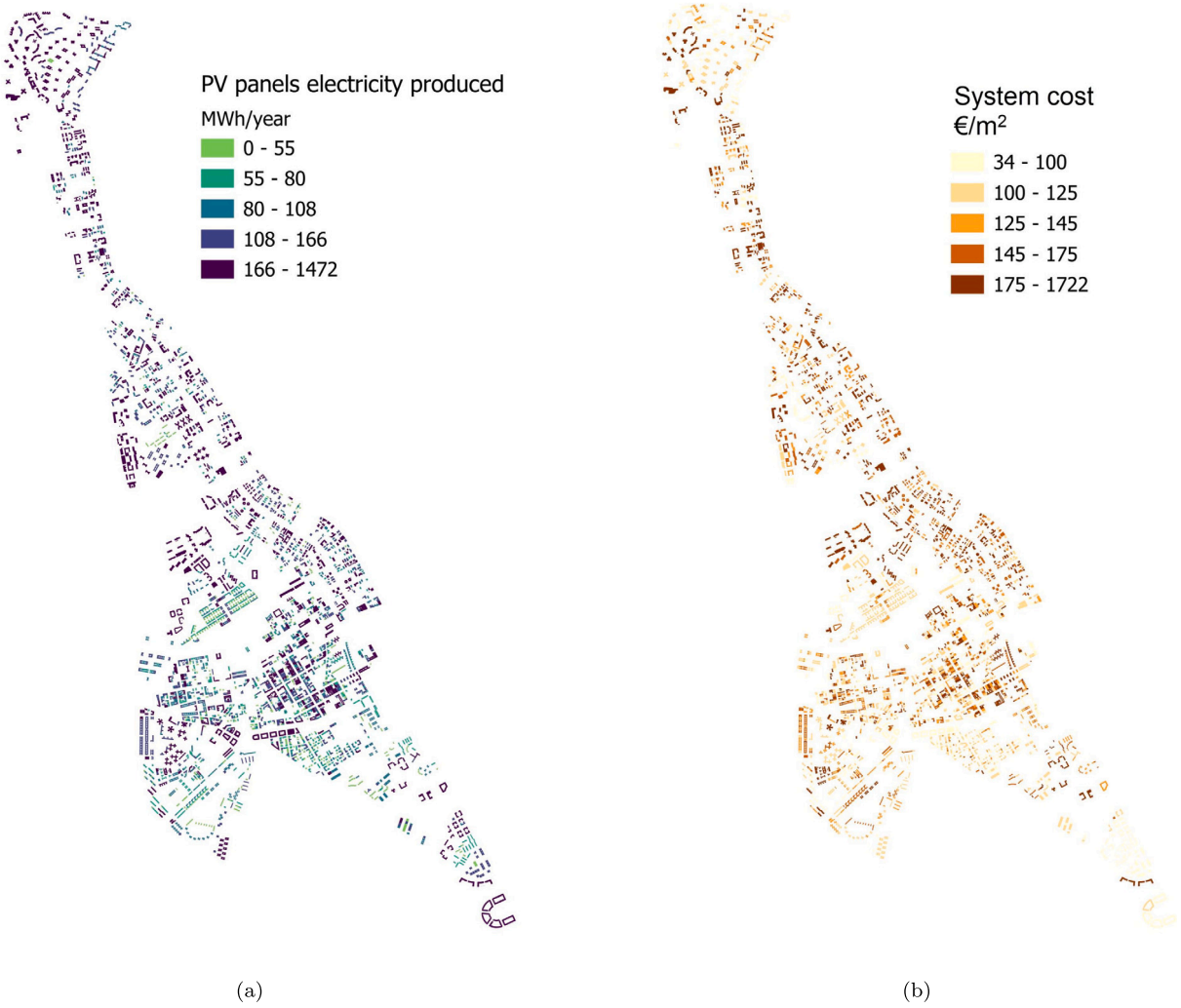

Fig. 6. (a). Maximum electricity produced per building according to its rooftop surface available.(b) Cost of the system (GSHP + PV) per building surface.

geothermal sources. Consequently, these 3,798 buildings were selected as suitable areas up to this point of the work.

3.2.3. Electricity production from PV

The computation of the maximum electricity available on selected buildings' rooftops was executed using Equation (3), employing Geographic Information System (GIS) tools. A combination of fixed and site-specific input data was utilized for this analysis. Fixed input parameters included a Performance Ratio of 0.8 and a utility lifetime of 25 years. A standard Power Peak of 1.1 kW was adopted for the system. Site-specific pixel data, comprised of solar irradiation values, is crucial for precise analysis and encapsulated in GIS format. This data, sourced from the "Digital Climatic Atlas of the Iberian Peninsula" [77], encompassed the entire region of Spain and Portugal. The Atlas provides digital climate maps of the Iberian Peninsula, detailing average air temperature, precipitation, and solar radiation every 200 meters annually and monthly. Rooftop surface data, essential for accurate calculations, was tailored to each building and was extracted from the Cadastral Database. An approximate method was employed, given the challenge of precisely estimating the available surface area for PV panels. This involved deducting 20% of the total surface area for potential shading losses and an additional 20% to accommodate the non-utilization of the entire surface. The annual solar radiation in the study locale amounted to 2,189 kWh/m^2 (optimum angle), with an average electricity generation rate of 0.34 MWh/m^2 per square meter of panel. This translates to an estimated total electricity output of approximately 404 MWh annually. On average, each building is projected to generate 106 MWh of electricity annually, with outputs ranging from 1 to 1,472 MWh per building, see Fig. 6a. These findings shed light on the considerable potential for electricity generation through rooftop PV installations, underscoring the significance of site-specific data in optimizing renewable energy strategies.

3.2.4. Coupled system cost

The system under consideration is designed to fulfill all of a building's heating needs. It comprises a Ground-Source Heat Pump (GSHP) with a specified number of Borehole Heat Exchangers (BHEs) to generate heat, complemented by Photovoltaic (PV) panels to generate the electricity required to power the GSHP.

Determining the optimal configuration involves several steps:

1. The requisite number of BHEs to satisfy the maximum heating demand of the building is determined beforehand.
2. The electricity consumption of the heat pump is calculated by dividing the heating demand by its Seasonal Coefficient of Performance (SCOP).
3. Once the necessary surface area for the PV panels and the length of BHEs have been established, the costs are computed by multiplying these parameters by predefined investment ratios. These ratios, €400/m^2 for the PV installation and €90/m for the GSHP installation, are derived from project budgets executed in Spain in recent years.

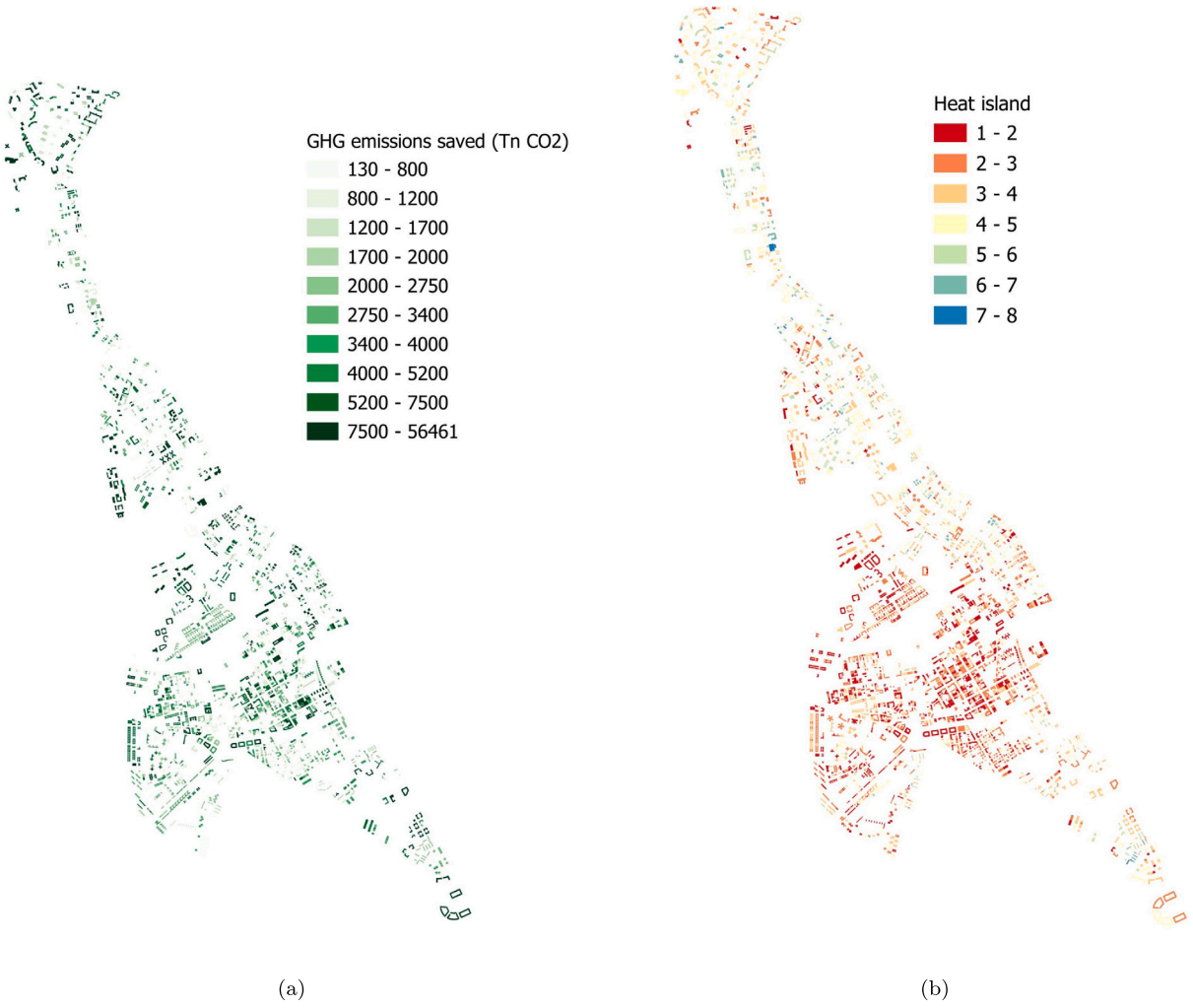

Fig. 7. (a). GHG saved (Tn CO_2).(b) Heat island index.

The analysis reveals that out of 3,798 surveyed buildings, 2,969 possess the capability to produce the total annual electricity demand required by the GSHP. This electricity demand spans a wide range, varying between 3 and 6,241 MWh, contingent upon each building's size and energy consumption profile. The incurred costs for implementing the system exhibit considerable variability, ranging from €24k to €38,060k across the selected buildings. Moreover, the system cost per square meter of the building ranges from €34 to €1,722, see Fig. 6b. These findings underscore the diverse economic implications associated with deploying systems tailored to individual building characteristics.

3.2.5. Emissions saved

The calculation of greenhouse gas (GHG) emissions saved hinges upon the electricity generated by each building and its subsequent multiplication by the emission factor of Spain's electricity mix in 2023, which stands at 273 gCO_{2eq}/kWh [78]. According to the analysis, buildings have the potential to mitigate GHG emissions by amounts ranging from 130 to around 57000 tons of CO_{2eq} annually, see Fig. 7a. Each building could save approximately 4000 tons of CO_{2eq} per year. Notably, nearly all buildings, almost 100% of them, exhibit emissions within the range of 1000 to 5000 tons, with 1,786 buildings exhibiting savings within this range. These findings underscore the substantial environmental benefits achievable through the adoption of renewable energy strategies like rooftop solar installations. By leveraging clean energy sources, buildings can play a pivotal role in curbing GHG emissions and contributing to a more sustainable future.

3.2.6. Heat island index

In 2022, the Madrid municipality introduced the Urban Climate Map [79]. This map, compiled from Landsat 8 satellite imagery, stems from a meticulous nine-month analysis, excluding periods of cloud cover. Utilizing a multi-criteria evaluation, it factors in diverse elements such as land and ambient temperatures, vegetation density, urban compactness, proximity to water bodies, slope, and shadows. Consequently, it delineates eight distinct thermal comfort levels, ranging from 1, representing extremely high, to 8, signifying very low. This innovative map serves as a pivotal tool in understanding the urban heat island effect. By overlaying it with the building layer, we elucidate the map's impact on the built environment. This amalgamation revealed a clear correlation: buildings with a higher heat island impact score correspond to areas ripe for investment in Ground Source Heat Pump (GSHP) technology to mitigate this effect effectively. Visual inspection of the resulting layer, see Fig. 7b, reveals conspicuous patterns. Notably, an intensely extreme heat island area emerges, aligning with the concentrated urban sprawl of Madrid's densely populated neighborhoods, particularly evident in the central-southern region. Here, transitioning to coupled heating systems presents a proactive solution to combat the heat island effect. Conversely, regions with a very low heat island index are discernible in select locations in the North and South, owing to their abundant green spaces.

4. Results & discussion

From phase 2, the decision matrix formed by the 6 criteria and 2,733 alternatives is obtained. Firstly, the weights of the criteria are obtained

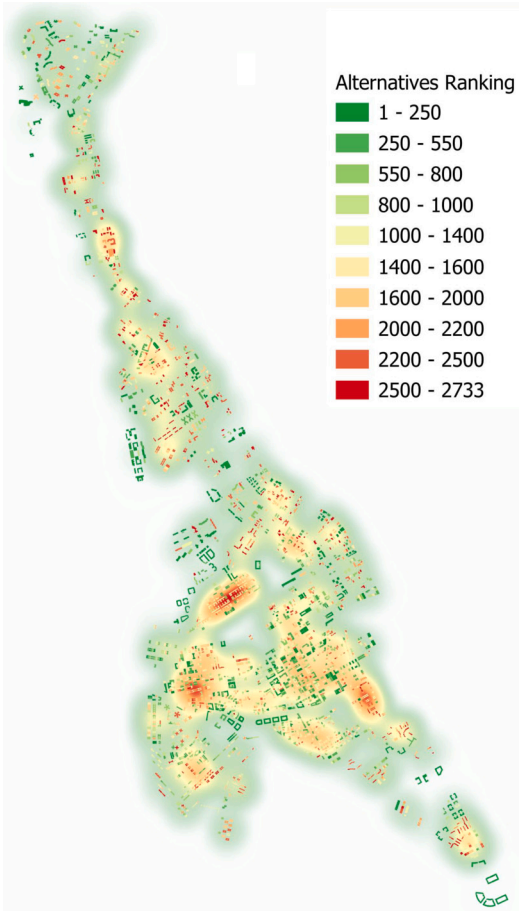

Fig. 8. Alternatives Ranking.

using the Entropy method 2.3.1, the predominant criterion turns out to be the savings of greenhouse gas (GHG) emissions with a weight of 17.11%, which is highly favorable in terms of the Sustainable Development Goal (SDG) number 13. The rest of the criteria do not exceed 17%, the production of photovoltaic energy (photovoltaic production), the heat island, BHE+PV cost, Age of the building and Energy demand of the building with 16.88%, 16.55%, 16.52%, 16.47% and 16.46% respectively. Finally, the ranking of alternatives is obtained using the VIKOR 2.3.1.

Based on the ranking of buildings according to their suitability for the PV-geothermal system (see Fig. 8), all buildings have been assessed and categorized from highly optimal (dark green) to less optimal (dark red). This ranking map is essential for identifying potential deployment areas for coupled PV-geothermal systems. A heatmap visualization highlights areas where less optimal alternatives are concentrated.

The most favorable zones (ranked 1-250) predominantly lie in the northern and central parts of the region, characterized by dark green shades, indicating favorable conditions for deployment. Conversely, the southern region shows a mix of moderately optimal to less optimal zones, with yellow, orange, and red areas signifying decreasing suitability. Therefore, initial investments in coupled PV-geothermal systems should prioritize these optimal green zones to maximize returns on investment and energy output, focusing efforts where conditions are most favorable

Considering this and advancing into Phase 3 of the methodology, four scenarios have been developed based on the optimized ranking derived from multi-criteria evaluation and the maximum annual investment feasible for the study area. The annual investment limits include the cost of systems corresponding to the ranking of alternatives (Fig. 8), determining the annual number of projects (alternatives) feasible within these financial constraints.

These scenarios also factor in anticipated annual subsidies from the IDAE (Spanish Institute for the Diversification and Saving of Energy) for heating and cooling via renewable energy sources, as well as electrical self-consumption in buildings. Given Madrid's representation of 14% of Spain's primary residences, where subsidies cover 40% of total investments, the scenarios vary based on different public investment percentages: 50%, 51 million euros per year total investment (S_1); 40%, 41 million euros per year total investment (S_2); 30%, 30 million euros per year total investment (S_3); and 20%, 20 million euros per year total investment (S_4).

By selecting the actions to be subsidized following the ranking obtained by applying the developed methodology, the number of buildings that can be intervened in each scenario during a period of 10 years has been obtained (Table 2). It is observed that in the scenarios with the lowest budget to invest (scenarios S_4, S_3), installations that represent greater energy savings and CO_2 emissions are prioritized, although they are more expensive unit investments, while the unit investment value decreases as the number of projects that can be carried out increases. The annual implementation of projects by scenario is represented in Fig. 9. The first buildings in the ranking involve considerable savings in CO_2 emissions and primary energy and a moderate cost, so taking into account the investment limit set for each scenario, the projects that can be executed during the first year achieve an important environmental improvement. The variations observed in the graphs during the following years are due to the fact that the implementation of the following buildings in the ranking requires a greater investment; hence, the number of projects to be executed annually decreases, reducing the total savings. At the end of the period, the buildings in the ranking have a lower investment cost, thus more projects can be implemented increasing the total savings. The objective of the methodology for building selection is more clearly observed in the graphs of CO_2 avoided emissions and primary energy savings by building. In all scenarios, except in some years in S_4 due to its low budget, it is observed how the implementation of the buildings that represent the most savings is prioritized.

5. Conclusions

The coupled system combining geothermal heat pumps (GSHP) and photovoltaic (PV) panels demonstrates both efficiency and viability for energy generation and greenhouse gas (GHG) emissions reduction in urban buildings. This system can meet the heating demand of buildings and generate the necessary electricity to operate the GSHPs, depending on the available surface area for PV installation. The economic impact of the system varies significantly according to the building characteristics and the surface area available for PV installation, with a wide range of costs from €24,000 to €38,060,000. The cost per square meter (34 - 1,772) also shows variability, reflecting the need for specific adaptations in each case. The analyzed buildings can reduce their GHG emissions in a range of 131 to 57 k metric tons of CO_2eq annually, with an average of 4 k metric tons of CO_2eq per building per year. Adopting renewable energy strategies, such as rooftop solar panel installations, can provide substantial environmental benefits, helping mitigate climate change and improving urban sustainability.

The developed tool for spatial planning of renewable coupled systems is useful for the efficient and sustainable planning of heating infrastructure in urban areas, considering the specific characteristics of each zone. To highlight that the presented tool is not a GHE or a PV design tool, to implement the installations in the buildings selected by the tool it will be necessary to carry out a detailed design. The methodology used, which includes geospatial analysis and multicriteria evaluation, allows for a detailed and adaptable assessment of different urban contexts. One of the main challenges is the assessment of interior building spaces, such as backyards, which the driller is unable to access, a fact that was not rigorously considered enough in this

Table 2
Energy refurbishment and investment scenarios.

	S_1	S_2	S_3	S_4
Annual Investment (M€)	51	41	30	20
Nº Projects (10 years)	599	339	160	70
Average investment per project (M€)	0.9	1.3	2.1	3.4
Total avoided emissions ($MtCO_2$/year)	5.0	3.7	2.6	1.6
Average avoided emissions ($ktCO_2$/year)	8.3	11.0	16.1	23.3
Total primary energy savings (GWh/year)	278.9	207.2	136.6	81.1
Average primary energy savings (MWh/year)	465.5	611.3	843.1	1158.8

Fig. 9. Total avoided emission [a]. Average avoided emissions [b]. Total primary energy savings [c]. Average primary energy saving [d].

study. Another challenge is the variability in costs and the availability of space for PV installation, which can affect the system's economic viability in certain buildings. Additionally, the inclination and orientation of roofs play a critical role in the economic returns of PV installations. For instance, roofs oriented towards the north often yield lower solar energy, thus providing reduced economic benefits. This factor can significantly influence the decision-making process for property owners and the overall feasibility of PV systems. Therefore, incorporating detailed spatial assessments of roof characteristics and orientation into future studies is essential to ensure a comprehensive evaluation of the potential for PV installations Integrating these technologies requires significant initial investment and careful planning to maximize economic and environmental benefits. Future research should consider the evolution of market prices for electricity and renewable technologies to improve the accuracy of economic assessments. It is also recommended to explore the integration of other renewable energy sources and emerging technologies that can complement and enhance the performance of coupled systems. Optimal locations show buildings where implement-

ing a ground-source heat pump driven by photovoltaic panels involves greater savings in primary energy and CO_2 emissions, helping prioritize sustainable investments. The developed methodology focuses on the coupled of heating systems but can be extended to cooling systems in future works. The database used to obtain the energy demand has limited this application, although the consideration of the heat island effect as a criterion introduces the selection of the most problematic locations to replace air condenser equipment with a geothermal closed loop in cooling mode. Energy demand in heating and cooling estimation using, for example, the EN-ISO 52016 standard constitutes a complete work in itself ([80]) therefore, it has been preferred to use databases of energy performance certificates, knowing their limitations, leaving this part for future methodology improvements. This study directly contributes to the Sustainable Development Goals (SDGs) 7 (affordable and clean energy), 11 (sustainable cities and communities), and 13 (climate action), providing a solid foundation for the development of public policies that promote the adoption of renewable technologies in urban environments.

CRediT authorship contribution statement

Adela Ramos-Escudero: Writing – review & editing, Writing – original draft, Visualization, Validation, Software, Methodology, Investigation, Formal analysis, Data curation, Conceptualization. **Teresa Magraner:** Writing – review & editing, Writing – original draft, Validation, Supervision, Resources, Methodology, Investigation, Data curation, Conceptualization. **Isabel C. Gil-García:** Writing – review & editing, Writing – original draft, Visualization, Supervision, Resources, Methodology, Investigation, Formal analysis, Data curation.

Declaration of competing interest

The authors declare that they have no known competing financial interests or personal relationships that could have appeared to influence the work reported in this paper.

Data availability

Data will be made available on request.

References

[1] M. Groll, Can climate change be avoided? Vision of a hydrogen-electricity energy economy, Energy 264 (2023) 126029, https://doi.org/10.1016/j.energy.2022.126029, https://www.sciencedirect.com/science/article/pii/S0360544222029152.

[2] V.Y. Mendez Angarita, L. Maiorano, C. Dragonetti, M. Di Marco, Implications of exceeding the Paris agreement for mammalian biodiversity, Conservation Science and Practice 5 (3) (2023) e12889, https://doi.org/10.1111/csp2.12889.

[3] Indicators of global climate change 2023: Annual update of key indicators of the state of the climate system and human influenceAvailable from, 2023 [Accessed 17th June 2024].

[4] Urban development overview, https://www.worldbank.org/en/topic/urbandevelopment/overview, 2023.

[5] Şiir Kılkış, Integrated urban scenarios of emissions, land use efficiency and benchmarking for climate neutrality and sustainability, Energy 285 (2023) 128643, https://doi.org/10.1016/j.energy.2023.128643, https://www.sciencedirect.com/science/article/pii/S0360544223020376.

[6] I.E.A. (IEA), Data and statistics, https://www.iea.org/data-and-statistics, 2023.

[7] R. International Energy Agency (IEA), International Renewable Energy Agency (IRENA), Renewable energy policies in a time of transition. Heating and cooling, Tech. Rep., 2020.

[8] G. Ulpiani, N. Vetters, D. Shtjefni, G. Kakoulaki, N. Taylor, Let's hear it from the cities: on the role of renewable energy in reaching climate neutrality in urban Europe, Renew. Sustain. Energy Rev. 183 (2023) 113444, https://doi.org/10.1016/j.rser.2023.113444, https://www.sciencedirect.com/science/article/pii/S1364032123003015.

[9] Home — United Nations sustainable development, https://www.un.org/sustainabledevelopment/.

[10] D. Gielen, F. Boshell, D. Saygin, M.D. Bazilian, N. Wagner, R. Gorini, The role of renewable energy in the global energy transformation, Energy Strategy Reviews 24 (2019) 38–50, https://doi.org/10.1016/j.esr.2019.01.006, https://www.sciencedirect.com/science/article/pii/S2211467X19300082.

[11] R.A. Evrin, I. Dincer, A novel multigeneration energy system for a sustainable community, in: I. Dincer, C.O. Colpan, M.A. Ezan (Eds.), Environmentally-Benign Energy Solutions, Springer International Publishing, Cham, 2020, pp. 557–584.

[12] S. Kavian, C. Aghanajafi, H. Jafari Mosleh, A. Nazari, A. Nazari, Exergy, economic and environmental evaluation of an optimized hybrid photovoltaic-geothermal heat pump system, Appl. Energy 276 (2020) 115469, https://doi.org/10.1016/j.apenergy.2020.115469, https://www.sciencedirect.com/science/article/pii/S0306261920309818.

[13] Y. Chen, J. Wang, P.D. Lund, Thermodynamic performance analysis and multi-criteria optimization of a hybrid combined heat and power system coupled with geothermal energy, Energy Convers. Manag. 210 (2020) 112741, https://doi.org/10.1016/j.enconman.2020.112741, https://www.sciencedirect.com/science/article/pii/S019689042030279X.

[14] A.G. Olabi, M. Mahmoud, B. Soudan, T. Wilberforce, M. Ramadan, Geothermal based hybrid energy systems, toward eco-friendly energy approaches, Renew. Energy 147 (2020) 2003–2012, https://doi.org/10.1016/j.renene.2019.09.140, https://www.sciencedirect.com/science/article/pii/S0960148119314843.

[15] Y. Chen, H. Hua, J. Wang, P.D. Lund, Integrated performance analysis of a space heating system assisted by photovoltaic/thermal collectors and ground source heat pump for hotel and office building types, Renew. Energy 169 (2021) 925–934, https://doi.org/10.1016/j.renene.2020.12.117, https://www.sciencedirect.com/science/article/pii/S0960148120320577.

[16] E. Hałaj, J. Kotyza, M. Hajto, G. Pełka, W. Luboń, P. Jastrzębski, Upgrading a district heating system by means of the integration of modular heat pumps, geothermal waters, and pvs for resilient and sustainable urban energy, Energies 14 (9) (2021), https://doi.org/10.3390/en14092347, https://www.mdpi.com/1996-1073/14/9/2347.

[17] M. Moldovan, B.-G. Burduhos, I. Visa, Yearly electrical energy assessment of a photovoltaic platform/geothermal heat pump prosumer, Energies 14 (13) (2021), https://doi.org/10.3390/en14133776, https://www.mdpi.com/1996-1073/14/13/3776.

[18] R. Neves, H. Cho, J. Zhang, Pairing geothermal technology and solar photovoltaics for net-zero energy homes, Renew. Sustain. Energy Rev. 140 (2021) 110749, https://doi.org/10.1016/j.rser.2021.110749, https://www.sciencedirect.com/science/article/pii/S1364032121000447.

[19] L. Perković, D. Leko, A.L. Brettschneider, H. Mikulčić, P.S. Varbanov, Integration of photovoltaic electricity with shallow geothermal systems for residential microgrids: proof of concept and techno-economic analysis with res2geo model, Energies 14 (7) (2021), https://doi.org/10.3390/en14071923, https://www.mdpi.com/1996-1073/14/7/1923.

[20] F. Ren, Z. Wei, X. Zhai, Multi-objective optimization and evaluation of hybrid cchp systems for different building types, Energy 215 (2021) 119096, https://doi.org/10.1016/j.energy.2020.119096, https://www.sciencedirect.com/science/article/pii/S0360544220322039.

[21] Y. Ruoping, Y. Xiangru, Y. Xiaohui, B. Yunpeng, W. Huajun, Performance study of split type ground source heat pump systems combining with solar photovoltaic-thermal modules for rural households in North China, Energy Build. 249 (2021) 111190, https://doi.org/10.1016/j.enbuild.2021.111190, https://www.sciencedirect.com/science/article/pii/S0378778821004746.

[22] Z. Changxing, X. Hang, L. Jiahui, L. Yufeng, P. Donggen, Operation characteristics of the composite system for combing solar pv/t collector and ground-coupled heat pump, https://doi.org/10.11975/j.issn.1002-6819.2021.12.025, 2021.

[23] M. Nahavandinezhad, A. Zahedi, Conceptual design of solar/geothermal hybrid system focusing on technical, economic and environmental parameters, Renew. Energy 181 (2022) 1110–1125, https://doi.org/10.1016/j.renene.2021.09.110, https://www.sciencedirect.com/science/article/pii/S0960148121014312.

[24] A. Allouhi, Techno-economic and environmental accounting analyses of an innovative power-to-heat concept based on solar pv systems and a geothermal heat pump, Renew. Energy 191 (2022) 649–661, https://doi.org/10.1016/j.renene.2022.04.001.

[25] M. Pilou, G. Kosmadakis, G. Meramveliotakis, A. Krikas, Towards a 100 with solar and geothermal energy, Sol. Energy Adv. 2 (2022) 100020, https://doi.org/10.1016/j.seja.2022.100020, https://www.sciencedirect.com/science/article/pii/S2667113122000080.

[26] J. Vourdoubas, Possibilities of using sustainable energy technologies including chp systems, solar photovoltaics and heat pumps in hospitals, J. Energy Res. 2 (2022) 1–8, https://doi.org/10.24018/ejenergy.2022.2.2.52, https://www.sciencedirect.com/science/article/pii/S2667113122000080.

[27] A. Mahmoudan, F. Esmaeilion, S. Hoseinzadeh, M. Soltani, P. Ahmadi, M. Rosen, A geothermal and solar-based multigeneration system integrated with a teg unit: development, 3e analyses, and multi-objective optimization, Appl. Energy 308 (2022) 118399, https://doi.org/10.1016/j.apenergy.2021.118399, https://www.sciencedirect.com/science/article/pii/S0306261921016354.

[28] H. Rostamnejad Takleh, V. Zare, F. Mohammadkhani, M. Sadeghiazad, Proposal and thermoeconomic assessment of an efficient booster-assisted cchp system based on solar-geothermal energy, Energy 246 (2022) 123360, https://doi.org/10.1016/j.energy.2022.123360, https://www.sciencedirect.com/science/article/pii/S0360544222002638.

[29] M. Herrando, D. Elduque, C. Javierre, N. Fueyo, Life cycle assessment of solar energy systems for the provision of heating, cooling and electricity in buildings: a comparative analysis, Energy Convers. Manag. 257

(2022) 115402, https://doi.org/10.1016/j.enconman.2022.115402, https://www.sciencedirect.com/science/article/pii/S0196890422001984.
[30] A.M. Al-Falahat, J.A. Qadourah, S.S. Alrwashdeh, R. khater, Z. Qatlama, E. Alddibs, M. Noor, Energy performance and economics assessments of a photovoltaic-heat pump system, Results Eng. 13 (2022) 100324, https://doi.org/10.1016/j.rineng.2021.100324, https://www.sciencedirect.com/science/article/pii/S2590123021001250.
[31] F. Calise, F.L. Cappiello, M. Dentice d'Accadia, F. Petrakopoulou, M. Vicidomini, A solar-driven 5th generation district heating and cooling network with ground-source heat pumps: a thermo-economic analysis, Sustain. Cities Soc. 76 (2022) 103438, https://doi.org/10.1016/j.scs.2021.103438, https://www.sciencedirect.com/science/article/pii/S2210670721007113.
[32] X. Sun, Y. Lin, Z. Zhu, J. Li, Optimized design of a distributed photovoltaic system in a building with phase change materials, Appl. Energy 306 (2022) 118010, https://doi.org/10.1016/j.apenergy.2021.118010, https://www.sciencedirect.com/science/article/pii/S0306261921013118.
[33] Z. Liu, X. Yang, H.M. Ali, R. Liu, J. Yan, Multi-objective optimizations and multi-criteria assessments for a nanofluid-aided geothermal pv hybrid system, Energy Rep. 9 (2023) 96–113, https://doi.org/10.1016/j.egyr.2022.11.170, https://www.sciencedirect.com/science/article/pii/S2352484722025586.
[34] X. Lü, T. Lu, S. Kariranne, A. Mäkiranta, D. Clements-Croome, Renewable energy resources and multi-energy hybrid systems for urban buildings in nordic climate, Energy Build. 282 (2023) 112789, https://doi.org/10.1016/j.enbuild.2023.112789, https://www.sciencedirect.com/science/article/pii/S0378778823000191.
[35] E. Baniasadi, M. Ziaei-Rad, M.A. Behvand, N. Javani, Exergy-economic analysis of a solar-geothermal combined cooling, heating, power and water generation system for a zero-energy building, Int. J. Hydrog. Energy 48 (99) (2023) 39064–39083, https://doi.org/10.1016/j.ijhydene.2023.01.186, Integrated Hydrogen Energy Systems, https://www.sciencedirect.com/science/article/pii/S0360319923003786.
[36] M. Kheir Abadi, V. Davoodi, M. Deymi-Dashtebayaz, A. Ebrahimi-Moghadam, Determining the best scenario for providing electrical, cooling, and hot water consuming of a building with utilizing a novel wind/solar-based hybrid system, Energy 273 (2023) 127239, https://doi.org/10.1016/j.energy.2023.127239, https://www.sciencedirect.com/science/article/pii/S0360544223006333.
[37] A. Sharifi, A. Eskandari, Techno-economic evaluation and multi-criteria optimization of a trigeneration flash–binary geothermal power plant integrated with parabolic trough solar collectors, J. Therm. Anal. Calorim. 148 (2023) 8263–8282, https://doi.org/10.1007/s10973-023-11968-x.
[38] M.E. Zayed, M.M. Aboelmaaref, M. Chazy, Design of solar air conditioning system integrated with photovoltaic panels and thermoelectric coolers: experimental analysis and machine learning modeling by random vector functional link coupled with white whale optimization, Therm. Sci. Eng. Prog. 44 (2023) 102051, https://doi.org/10.1016/j.tsep.2023.102051, https://www.sciencedirect.com/science/article/pii/S2451904923004043.
[39] G. Liu, D. Ji, Y. Qin, Geothermal-solar energy system integrated with hydrogen production and utilization modules for power supply-demand balancing, Energy 283 (2023) 128736, https://doi.org/10.1016/j.energy.2023.128736, https://www.sciencedirect.com/science/article/pii/S0360544223021308.
[40] N. Sommerfeldt, J.M. Pearce, Can grid-tied solar photovoltaics lead to residential heating electrification? A techno-economic case study in the midwestern U.S., Appl. Energy 336 (2023) 120838, https://doi.org/10.1016/j.apenergy.2023.120838, https://www.sciencedirect.com/science/article/pii/S0306261923002027.
[41] H. Kim, L. Junghans, Economic feasibility of achieving net-zero emission building (nzeb) by applying solar and geothermal energy sources to heat pump systems: a case in the United States residential sector, J. Clean. Prod. 416 (2023) 137822, https://doi.org/10.1016/j.jclepro.2023.137822, https://www.sciencedirect.com/science/article/pii/S0959652623019807.
[42] Y. Altork, M.I. Alamayreh, Optimizing hybrid heating systems: identifying ideal stations and conducting economic analysis heating houses in Jordan, International Journal of Heat and Technology 42 (2024) 529–540, https://doi.org/10.18280/ijht.420219.
[43] M. Krarouch, A. Allouhi, H. Hamdi, A. Outzourhit, Energy, exergy, environment and techno-economic analysis of hybrid solar-biomass systems for space heating and hot water supply: case study of a hammam building, Renew. Energy 222 (2024) 119941, https://doi.org/10.1016/j.renene.2024.119941, https://www.sciencedirect.com/science/article/pii/S0960148124000065.
[44] A. Shahee, M. Abdoos, A. Aslani, R. Zahedi, Reducing the energy consumption of buildings by implementing insulation scenarios and using renewable energies, Energy Inf. 7 (2024) 18, https://doi.org/10.1186/s42162-024-00311-9.
[45] J. Li, L. Bao, G. Niu, Z. Miao, X. Guo, W. Wang, Research on renewable energy coupling system based on medium-deep ground temperature attenuation, Appl. Energy 353 (2024) 122187, https://doi.org/10.1016/j.apenergy.2023.122187, https://www.sciencedirect.com/science/article/pii/S0306261923015519.
[46] A. Billerbeck, C. Bernath, P. Manz, G. Deac, A. Held, J. Winkler, A. Kök, M. Ragwitz, Integrating district heating potentials into European energy system modelling: an assessment of cost advantages of renewable and excess heat, Smart Energy 15 (2024) 100150, https://doi.org/10.1016/j.segy.2024.100150, https://www.sciencedirect.com/science/article/pii/S2666955224000200.
[47] Z. Wang, S. Li, W. Cai, P. Li, J. Deng, Strategy and capacity optimization of renewable hybrid combined cooling, heating and power system with multiple energy storage, Appl. Therm. Eng. 242 (2024) 122499, https://doi.org/10.1016/j.applthermaleng.2024.122499, https://www.sciencedirect.com/science/article/pii/S1359431124001674.
[48] J. Zhu, T.U. Kumar Nutakki, P.K. Singh, B.S. Abdullaeva, X. Zhou, Y. Fouad, L.H. Alzubaidi, Sustainable off-grid residential heating and desalination: integration of biomass boiler and solar energy with environmental impact analysis, J. Build. Eng. 87 (2024) 109035, https://doi.org/10.1016/j.jobe.2024.109035, https://www.sciencedirect.com/science/article/pii/S235271022400603X.
[49] J. Li, Y. Ren, X. Ma, Q. Wang, Y. Ma, Z. Yu, J. Li, M. Ma, J. Li, Comprehensive evaluation of the working mode of multi-energy complementary heating systems in rural areas based on the entropy-topsis model, Energy Build. 310 (2024) 114077, https://doi.org/10.1016/j.enbuild.2024.114077, https://www.sciencedirect.com/science/article/pii/S0378778824001932.
[50] W.-L. Shang, Z. Lv, Low carbon technology for carbon neutrality in sustainable cities: a survey, Sustain. Cities Soc. 92 (2023) 104489, https://doi.org/10.1016/j.scs.2023.104489, https://www.sciencedirect.com/science/article/pii/S2210670723001002.
[51] A. Marvuglia, L. Havinga, O. Heidrich, J. Fonseca, N. Gaitani, D. Reckien, Advances and challenges in assessing urban sustainability: an advanced bibliometric review, Renew. Sustain. Energy Rev. 124 (2020) 109788, https://doi.org/10.1016/j.rser.2020.109788, https://www.sciencedirect.com/science/article/pii/S1364032120300848.
[52] Welcome to the qgis project!, https://qgis.org/en/site/index.html#.
[53] Welcome — trnsys: Transient system simulation tool, https://www.trnsys.com/.
[54] Energyplus, https://energyplus.net/.
[55] Esp-r — university of strathclyde, https://www.strath.ac.uk/research/energysystemsresearchunit/applications/esp-r/.
[56] C. Tissen, K. Menberg, P. Bayer, P. Blum, Meeting the demand: geothermal heat supply rates for an urban quarter in Germany, Geotherm. Energy 7 (1) (2019) 9, https://doi.org/10.1186/s40517-019-0125-8.
[57] L. Serrano-Luján, N. Espinosa, J. Abad, A. Urbina, The greenest decision on photovoltaic system allocation, Renew. Energy 101 (2017) 1348–1356, https://doi.org/10.1016/j.renene.2016.10.020, https://www.sciencedirect.com/science/article/pii/S0960148116308850.
[58] S.K. Sahoo, S.S. Goswami, A comprehensive review of multiple criteria decision-making (mcdm) methods: advancements, applications, and future directions, Decision Making Advances 1 (1) (2023) 25–48, https://doi.org/10.31181/dma1120237, https://www.dma-journal.org/index.php/dema/article/view/7.
[59] P.A. Alvarez, A. Ishizaka, L. Martínez, Multiple-criteria decision-making sorting methods: a survey, Expert Syst. Appl. 183 (2021) 115368, https://doi.org/10.1016/j.eswa.2021.115368, https://www.sciencedirect.com/science/article/pii/S0957417421007958.
[60] M. Zeleny, Multiple criteria decision making, 1982.
[61] F. Sitorus, P.R. Brito-Parada, A multiple criteria decision making method to weight the sustainability criteria of renewable energy technologies under uncertainty, Renew. Sustain. Energy Rev. 127 (2020) 109891, https://doi.org/10.1016/j.rser.2020.109891, https://www.sciencedirect.com/science/article/pii/S1364032120301842.
[62] A. Hashemi, M.B. Dowlatshahi, H. Nezamabadi-pour, Vmfs: a vikor-based multi-target feature selection, Expert Syst. Appl. 182 (2021) 115224, https://doi.org/10.1016/j.eswa.2021.115224, https://www.sciencedirect.com/science/article/pii/S0957417421006564.
[63] B. Paradowski, A. Bączkiewicz, J. Watrąbski, Towards proper consumer choices - mcdm based product selection, Proc. Comput. Sci. 192 (2021) 1347–1358, https://doi.org/10.1016/j.procs.2021.08.138, Knowledge-Based and Intelligent Information & Engineering Systems: Proceedings of the 25th International Conference KES2021, https://www.sciencedirect.com/science/article/pii/S1877050921016276.
[64] M. de Vivienda y Agenda Urbana, Ficheros de datos climáticos cte db-he, https://www.codigotecnico.org/DocumentosCTE/AhorroEnergia.html, 2016.
[65] Madrid Municipality Open Data, https://datos.madrid.es/portal/site/egob/menuitem.c05c1f754a33a9fbe4b2e4b284f1a5a0/?vgnextoid=a4f36d34fa86c410VgnVCM2000000c205a0aRCRD&vgnextchannel=374512b9ace9f310VgnVCM100000171f5a0aRCRD.
[66] AENOR, Diseño, ejecución y seguimiento de una instalación geotérmica somera, Parte 1: Sistemas de circuito cerrado vertical (une 100715-1), 2014.
[67] Ministerio de Hacienda, Gobierno de España, Sede electrónica del catastro, https://www.sedecatastro.gob.es/, 2020.
[68] M. para la transformación digital y de la función pública, Urban3r plataforma de datos abiertos para la regeneración urbana en españa, https://urban3r.es, 2023.
[69] E. Parliament, Directive (eu) 2018/844 of the European Parliament and of the council of 30 may 2018 amending directive 2010/31/eu on the energy performance of buildings and directive 2012/27/eu on energy efficiency (text with eea relevance), http://data.europa.eu/eli/dir/2018/844/oj, 2018.
[70] P. del Gobierno, Real decreto 2429/1979. Norma básica de edificación nbe-ct-79, sobre condiciones térmicas en los edificios, https://www.boe.es/eli/es/rd/1979/07/06/2429, 1979.
[71] M. de Vivienda, Real decreto 214/2006. Código técnico de la edificación, https://www.boe.es/buscar/doc.php?id=BOE-A-2006-5515, 2006.
[72] M. de Fomento, Real decreto 732/2019, de 20 de diciembre, por el que se modifica el código técnico de la edificación, aprobado por el real decreto 314/2006, de 17 de marzo, https://www.boe.es/diario_boe/txt.php?id=BOE-A-2019-18528, 2019.
[73] I. para la Diversificación y el Ahorro de la Energía (IDAE), Evaluación del potencial de energía geotérmica. Estudio técnico per 2011-2020, 2011.

[74] E.E. Designer, https://buildingphysics.com/eed-2/.
[75] T. Başer, J.S. McCartney, Y. Dong, N. Lu, Evaluation of coupled thermal and hydraulic relationships used in simulation of thermally-induced water flow in unsaturated soils, pp. 370–380, https://doi.org/10.1061/9780784481691.037, https://ascelibrary.org/doi/pdf/10.1061/9780784481691.037, https://ascelibrary.org/doi/abs/10.1061/9780784481691.037.
[76] I. para la Diversificación y el Ahorro de la Energía (IDAE), Frecuencias horarias de repetición en temperatura. Intervalo 24 h, 2014.
[77] M. Ninyerola, X. Pons, J. Roure, Atlas climático digital de la península ibérica. Metodología y aplicaciones en bioclimatología y geobotánica, Universidad Autónoma de Barcelona, Bellaterra, 2005, ISBN 932860-8-7, https://opengis.grumets.cat/wms/iberia/portugues/po_model.htm.
[78] Comisión Nacional de los Mercados y la Competencia, Mercado eléctrico (fecha de acceso), https://www.cnmc.es/ambitos-de-actuacion/energia/mercado-electrico.
[79] Ayuntamiento de Madrid, Heat island map Madrid (fecha de acceso), https://geoportal.madrid.es/IDEAM_WBGEOPORTAL/dataset.iam?id=3ffba0d0-5ba2-4051-8a52-954b8b540207.
[80] C. Prades-Gil, J. Viana-Fons, X. Masip, A. Cazorla-Marín, T. Gómez-Navarro, An agile heating and cooling energy demand model for residential buildings. Case study in a Mediterranean city residential sector, Renew. Sustain. Energy Rev. 175 (2023) 113166, https://doi.org/10.1016/j.rser.2023.113166, https://www.sciencedirect.com/science/article/pii/S1364032123000229.